Available online at www.sciencedirect.com
SCIENCE DIRECT®
Sedimentary Geology 156 (2003) 95–118
Sedimentary Geology
www.elsevier.com/locate/sedgeo

Northern Caucasus basin: thermal history and synthesis of subsidence models

Andrey V. Ershov [a,*], Marie-Françoise Brunet [b], Anatoly M. Nikishin [a], Sergey N. Bolotov [a], Bronislav P. Nazarevich [a], Maxim V. Korotaev [a]

[a] *Regional Geology and Earth History Department, Geological Faculty, Moscow State University, Vorobievy Gory, 119899 Moscow, Russia*
[b] *UMR 7072 Tectonique CNRS-UPMC, case 129, University Pierre and Marie Curie, 4 place Jussieu, 75252 Paris Cedex 05, France*

Received 12 December 1999; received in revised form 11 September 2000; accepted 19 July 2002

Abstract

Burial histories of the eastern, central and western parts of the Northern Caucasus basin are reconstructed on the basis of well data and seismic sections. Subsidence began in the Early Triassic after the Late Carboniferous–Permian orogeny. Triassic sediments were mainly removed during Late Triassic–Early Jurassic uplift and erosion. Platform cover began to form in the Middle Jurassic and Albian sediments covered the whole territory of the basin. Thermal modelling shows that Jurassic–Eocene subsidence was mainly controlled by Late Triassic–Early Jurassic intrusive warming. This heating event induced thermal uplift of the whole territory followed by exponentially decelerating subsidence due to cooling of the lithosphere. In the southern areas adjacent to Great Caucasus, subsidence was also affected by Caucasian extensional and compressional events. In the Oligocene–Early Miocene, the eastern and the central basins underwent rapid long wavelength subsidence (Maikopian subsidence). The geodynamic cause of this subsidence is probably associated with the mantle flow appearance after cessation of the Tethyan subduction, due to reequilibration of subducted slab. While in the Late Miocene–Quaternary times, the eastern and the western basins underwent foreland-type asymmetrical subsidence due to loading of the Great Caucasus orogen; the central basin was uplifted. According to flexural modelling, the main component of orogen loading was the lithospheric root load; delamination of the latter under the Central Caucasus caused rapid uplift of the orogen and adjacent basin.

Keywords: Caucasus; Northern Caucasus basin; Burial history; Thermal history; Subsidence; Geodynamical model

1. Introduction

The Northern Caucasus basin (NCB) (also called Fore-Caucasus or Ciscaucasus) has been studied during more than 100 years since oil discovery times at the end of the last century. Geological literature on NCB consists of several hundred works, mainly in Russian. In English, tectonics and the geological history of the region were described by Borsuk and Sholpo (1983), Gamkrelidze (1986), Zonenshain and Le Pichon (1986), Philip et al. (1989), Adamia et al. (1992), Nikishin et al. (1998a,b), and Kopp and Scherba (1998).

In contrast with geological investigations, modelling studies were not numerous. Early models were general and equally applicable to many basins in the world. Regional numerical modelling, aimed at ex-

* Corresponding author. Tel.: +7-95-9393865; fax: +7-95-9328889.
E-mail address: and@geol.msu.ru (A.V. Ershov).

0037-0738/02/$ - see front matter © 2002 Elsevier Science B.V. All rights reserved.
PII: S0037-0738(02)00284-1

plaining the details of stratigraphy and tectonics of the specific basin, was not carried out until the 1980s. Amongst the first works were those of Mikhailov (1993), who carried out palaeotectonic analysis of Terek-Caspian basin; Ruppel and McNutt (1990), who modelled gravity anomalies and estimated effective elastic thickness of the lithosphere, and Bolotov (1996), who presented an analysis of basin subsidence history on the basis of 129 backstripped wells. Ershov et al. (1998, 1999) and Mikhailov et al. (1999a) published burial history restorations of NCB. There were several geodynamic models proposed for the Late Cainozoic collisional stage. The model of Artyushkov (1993) supposes a basalt–eclogite phase transition in the lower crust as the driving force of the foreland basin subsidence and orogen uplift. Mikhailov et al. (1999b) explained basin subsidence by a viscous flow in the crust. Ershov et al. (1999) adopted the flexural model of foreland basin and determined the main types of orogen loading in the Caucasus case.

Here, we complete these studies by thermal model explaining the subsidence of the Jurassic–Eocene stage, by the kinematic analysis of the collision and, finally, present a synthesis of the subsidence models throughout the basin evolution.

2. Structural settings

2.1. Recent tectonic environment

The Caucasus region is a part of the Alpine–Himalayan orogenic belt, located between the Black Sea and the Caspian Sea. Tectonically, it can be subdivided into the Great Caucasus (GC) orogen, the western (Indol-Kuban) and the eastern (Terek-Caspian) Northern Caucasus molasse basins (NCB) separated by the basement uplift of the Stavropol High; and, finally, the western (Rioni) and the eastern (Kura) Transcaucasus molasse basins (Fig. 1a). These latter basins are bounded by the arcuate Lesser Caucasus mountains and opened respectively towards the Black Sea and the South Caspian Sea. The GC orogen is a northwest trending nearly linear structure. The linearity of the GC is mainly explained by the right-lateral transpressional environment of its formation (Nikishin et al., 2003). Structurally, it is the deformed southern margin of the Late Palaeozoic Scythian Platform which extends along the southern margin of the Russian Platform. The Scythian Platform is bounded on the north by the Karpinsky Swell, which formerly was a part of the Dnieper–Donets–Karpinsky rift system (Nikishin et al., 1996), and now is the peripheral bulge of the Northern Caucasus molasse basin. The deepest parts of the NCB are the Terek-Caspian depression for the east and the Indol-Kuban depression for the west.

A scheme of the recent tectonic environment of the Caucasus region is presented in Fig. 1b. It is mainly determined by the indention of Arabia, induced lateral expulsion of the rigid Anatolian and Iranian plates and distributed deformation in the broad area situated between the Arabian margins and the GC orogen. The present-day Arabian velocity in Eurasia-fixed reference frame is equal to 25 ± 3 mm/year (N38) according to NUVEL-1A model (De Mets et al., 1990) in general coincidence with the 18–20 mm/year of recent geodetic observations (Smith et al., 1994; Reilinger et al., 1997a; McClusky et al., 2000). GPS observations show a minimum shortening of 10 ± 2 mm/year in the area of the Great and Lesser Caucasus (Reilinger et al., 1997b; McClusky et al., 2000).

2.2. Crustal structure

The main sources of information about the crustal structure of the region are the deep seismic data acquired more than 20 years ago. There are no new published high-resolution deep seismic sounding (DSS) sections in this region. Existing data have not enough resolution to show details of the crustal structure under the GC orogen and in the Transcaucasus areas.

Three synthetic sections representing crustal structure of the Caucasus and its molasse basins are displayed in Fig. 2, their locations are shown by the grey lines on Fig. 1a. The first section (line A) is totally synthetic. It was constructed on the basis of Moho map (Volvovsky et al., 1989), deep seismic section of Robinson et al. (1996) in the Black Sea and seismic section in the Western Fore-Caucasus basin (it is presented in the next section of this paper; Fig. 6). The two other sections are based on the DSS sections Stepnoe–Bakuriani (line B) and Volgograd–Nakhichevan (line C) crossing out the central and eastern parts of the region. Geophysical processing of crustal sections B and C was done by Krasnopevtseva (1984).

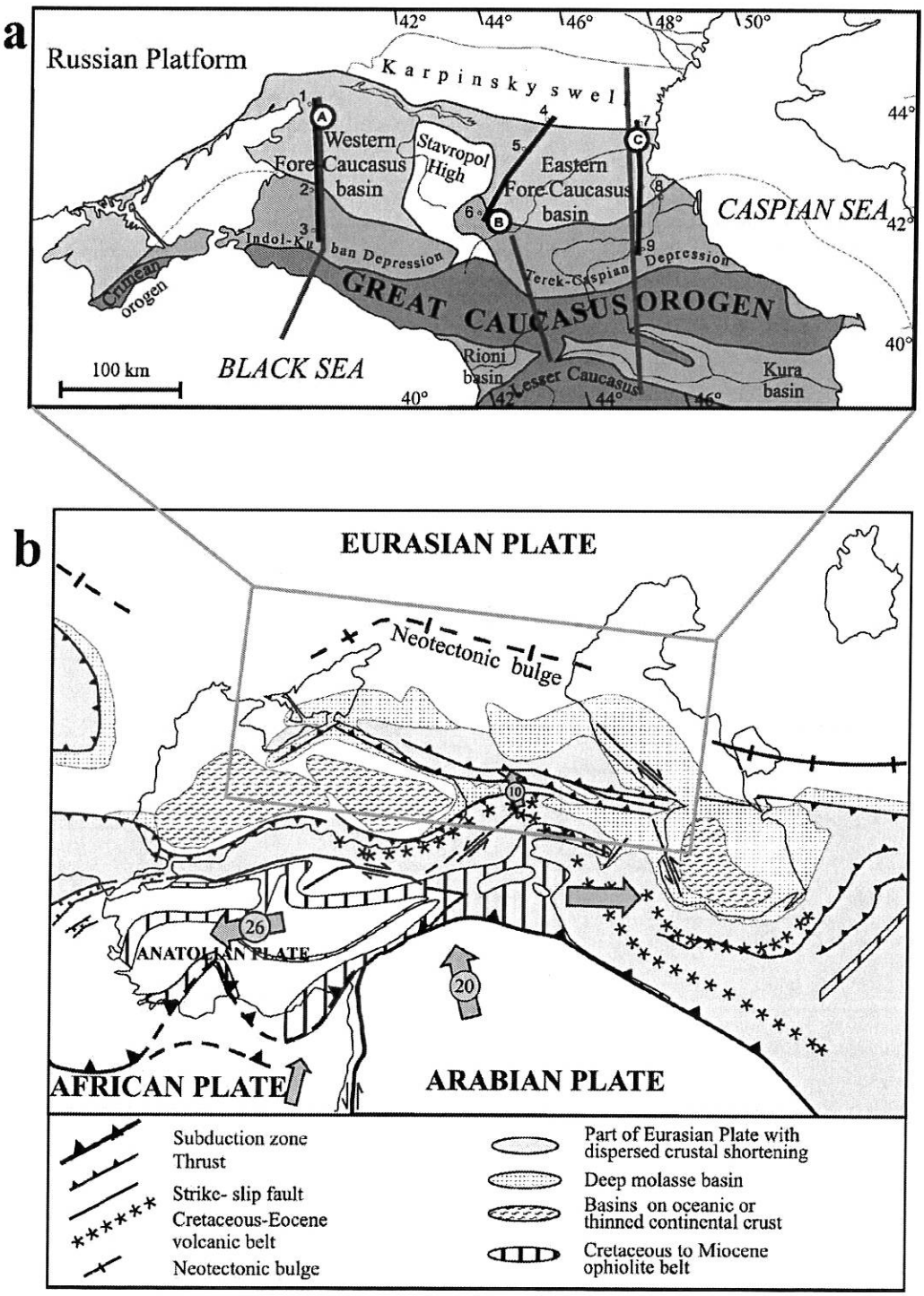

Fig. 1. (a) Schematic map of the investigated area showing positions of backstripped pseudo-wells (circles), seismic sections (black lines), and crustal-scale synthetic sections (grey lines). (b) Present-day tectonic setting of the Caucasus region. The plate velocities (mm/year, in Eurasia fixed framework) and shortening values are shown on the basis of geodetic observations (Reilinger et al., 1997a,b).

Geological data resulting from field observations in orogenic areas, and from seismic and well data in basinal areas were used to construct the upper parts of the sections.

Seismic data permit the recognition of four layers in the Scythian Platform crust: (1) Jurassic–Quaternary sediments; (2) Palaeozoic basement (Hercynian with Triassic inclusions (Letavin, 1980)) (seismic velocities 5.3–6.0 km/s); (3) Precambrian folded rocks with seismic velocities 6.0–6.6 km/s; (4) lower crust with seismic velocities 6.8–7.2 km/s. Sediments are well investigated by numerous wells and explora-

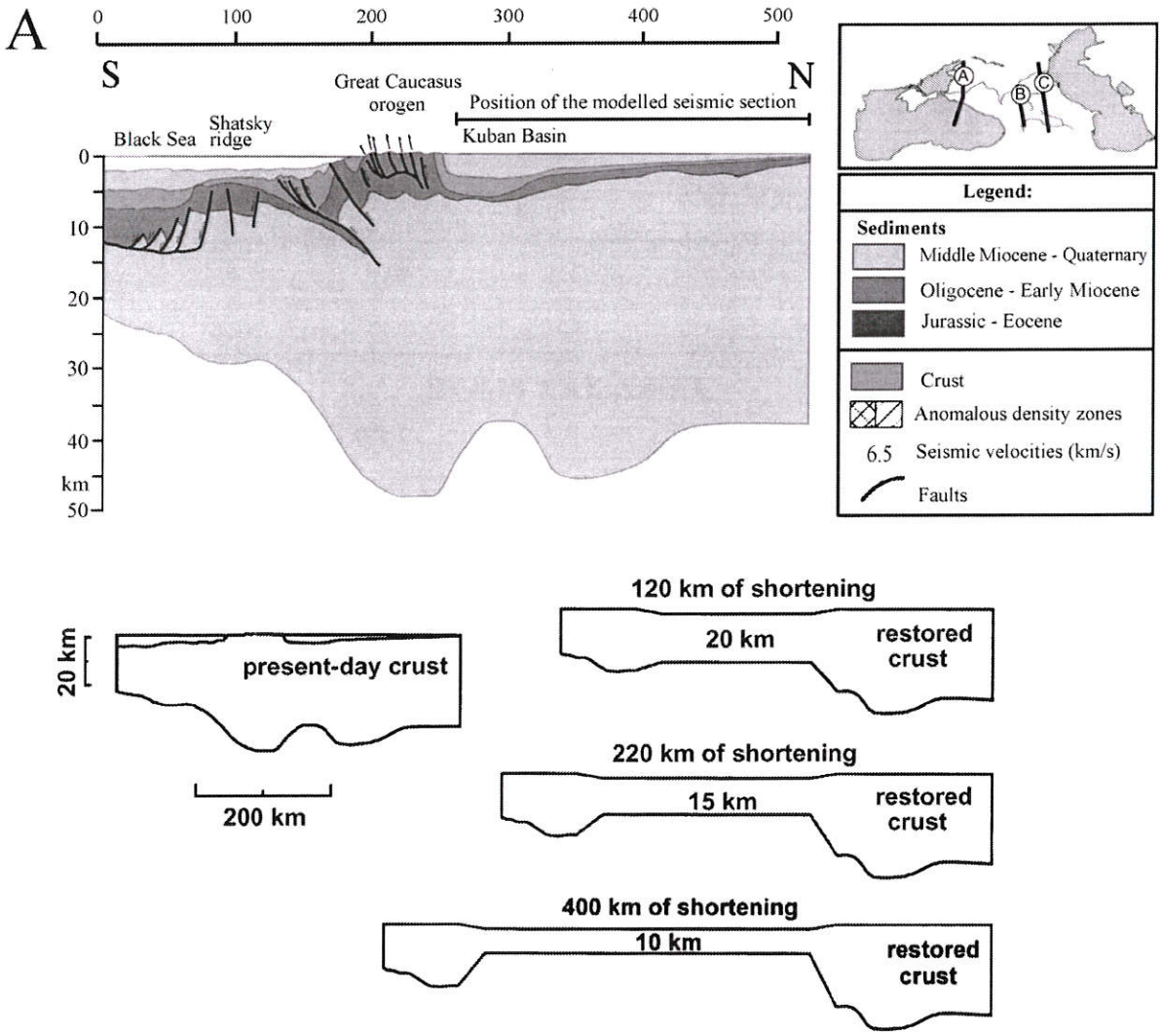

Fig. 2. Crustal scale synthetic sections through the Western Caucasus (A), Central Caucasus (B) and Eastern Caucasus (C) areas. Positions of the synthetic sections are shown in Fig. 1 (grey lines). Section A is constructed from the section of Robinson et al. (1996) in the Black Sea, the Moho map of Volvovsky et al. (1989) and seismic section in the Western Caucasus basin. The other two sections are drawn on the basis of deep seismic sections Stepnoe-Bakuriani (B) Volgograd-Nakhichevan (C) (modified after Krasnopevtseva, 1984). The upper parts are constructed on the basis of field geological data in the area of the orogen and from seismic and well data in basins. Stars mark the epicentres of large earthquakes. Lower sketches present the results of equal area restorations of crustal thickness. Initial configurations are taken from the observed sections, restored configurations are constructed giving them simplified form and equalizing the areas of initial and restored sections. As pre-deformational crustal thickness of the Great Caucasus trough is unknown, three possible values (maximum—20 km, minimum—10 km and intermediate—15 km) were used. Restorations are utilized to constrain shortening.

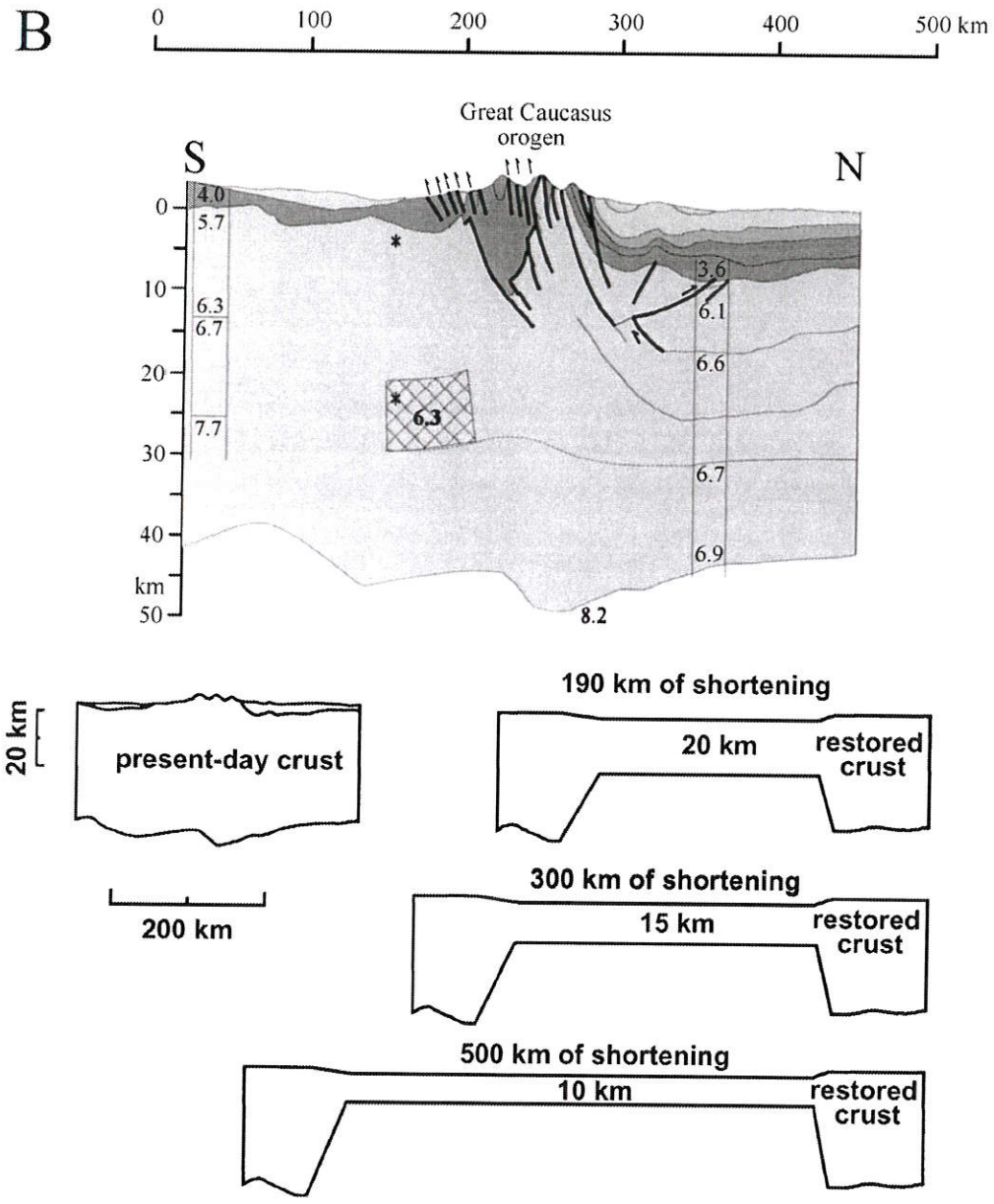

Fig. 2 (*continued*).

tion seismic sections. Palaeozoic rocks of the second seismic layer are penetrated by wells in some areas (Letavin, 1980). To the north, the bottom of this layer is correlated with the bottom of Palaeozoic sediments of the Russian Platform; towards the GC this layer is thinned out (Krasnopevtseva, 1984). The third seismic layer is traced on the DSS section Stepnoe–Bakuriani (line B) to the surface, where Precambrian crystalline metamorphic schists, gneisses and Hercynian granitic intrusions are outcropping (Krasnopevtseva, 1984). The thickness of the Scythian platform crust (without sediments) is around 40 km and decreases to near 30 km below the Terek-Caspian and Indol-Kuban basins. Low velocity zones are located under the GC orogen and Karpinsky swell-areas of recent uplift.

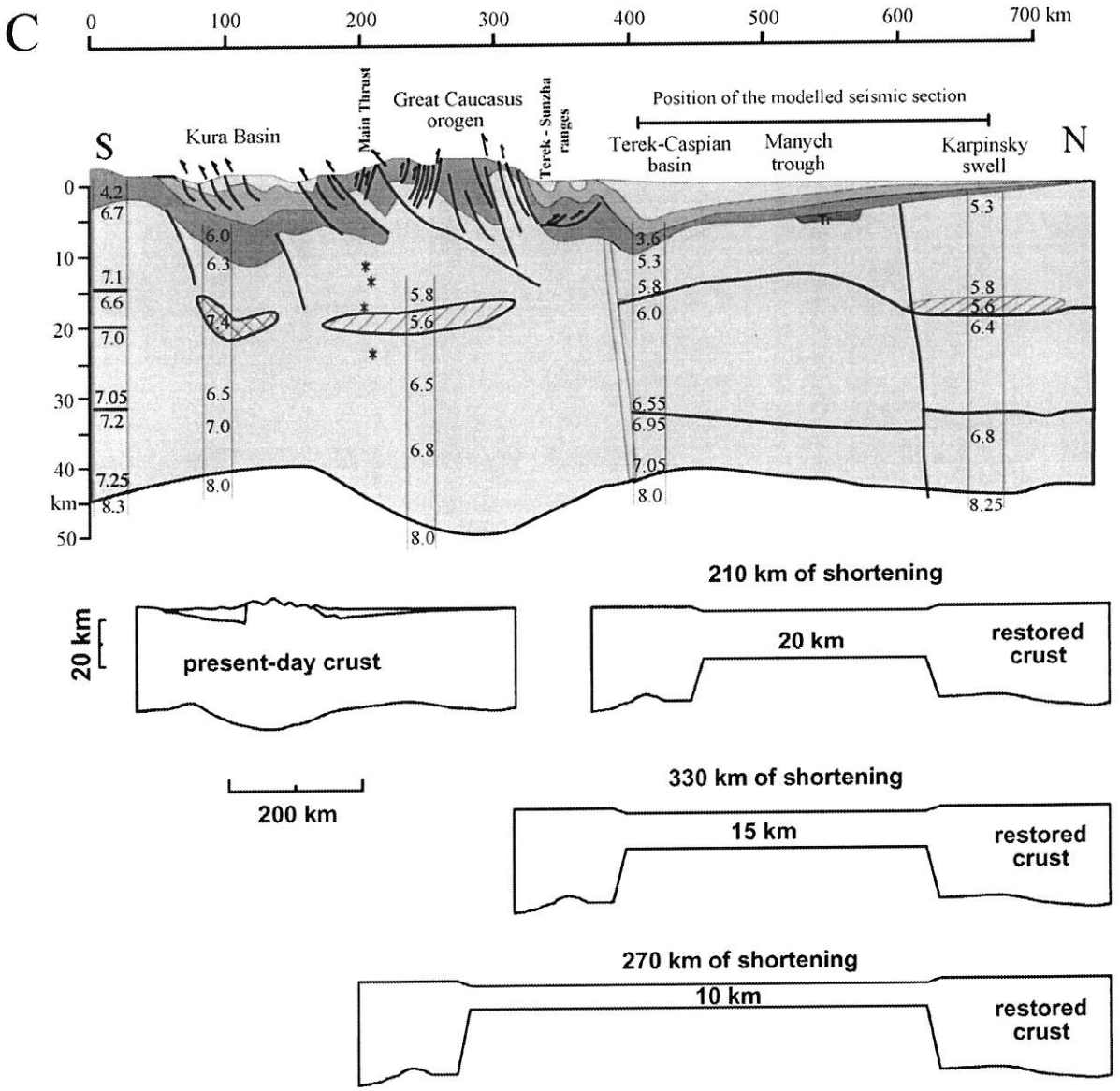

Fig. 2 (*continued*).

In the Transcaucasus area, the basement has mainly Proterozoic age; the second seismic layer is absent. In the area of the southern slope of the GC, the upper crust is layered and expressed by higher seismicity. The crustal structure of the Kura basin is characterised by numerous multidirectional reflectors, diffraction points and seismic focuses, probably due to numerous mantle intrusions in the upper part of the crust. A high velocity zone is present under the Kura basin. Kura basin is the western onshore part of the South Caspian Basin (see Brunet et al., 2003).

2.3. Architecture of the orogen and the basins

The GC orogen is upthrusted mainly to the south towards the Transcaucasus basins, with local retro-thrusting to the north. It was formed by the deformation of the Scythian and the Transcaucasus plates and

intermediate depression. The southern edge of the Scythian plate is expressed by the main thrust (Fig. 2C). The northern boundary of the Transcaucasus plate is overridden by the Scythian plate and folded sediments of the southern slope of the GC. These sediments initially were lying in an intermediate basin (the Great Caucasus trough). The northern slope of the GC is characterised by more simple tectonic styles: monocline transition to the Scythian Platform (central part, Fig. 2B), retro-thrusting to molasse basin (eastern part, Fig. 2C) or steep monocline transition to molasse basin with local retrothrusting (western part, Fig. 2A). The Northern Caucasus molasse basins have an asymmetrical shape with deepening towards the orogen and shallowing to the foreland. Along the southern boundary of the Terek-Caspian depression, the northern slope of GC orogen is overthrusted on the basin along the retro-thrusts (Fig. 2C). The Transcaucasus basins have a similar shape with deepening to the orogen, though they are faulted by numerous south-vergent thrusts.

2.4. Shortening during the Late Cainozoic collision

Here we give some estimations of the Caucasus shortening, which is one of the most disputed problems in Caucasus geology. Estimations of shortening range from a minimum value of 50–90 km observed shifts along thrust surfaces (Khain, 1982), to 900 km proposed by Bazhenov and Burtman (1990) on the basis of palaeomagnetic data. However, palaeomagnetic estimations should be considered with great care, because they imply shortening in the area situated to the north of the Great Caucasus (Westphal et al., 1986; Bazhenov and Burtman, 1990) and not between the Lesser Caucasus and the Great Caucasus, as field geology testifies.

The upper limit of the shortening value is provided by global plate kinematics. Fig. 3 represents the trajectory of Arabia relative to Eurasia's movement. The total shortening, since the beginning of collision (Oligocene to Quaternary), is about 400 km. Part of it was accommodated by Anatolia's lateral expulsion and another part (at present time—about half, according to geodetic data of Reilinger et al., 1997b and McClusky et al., 2000) corresponds to a shortening in the Caucasus area. In this way, the Caucasus's shortening can be estimated to 100–300 km.

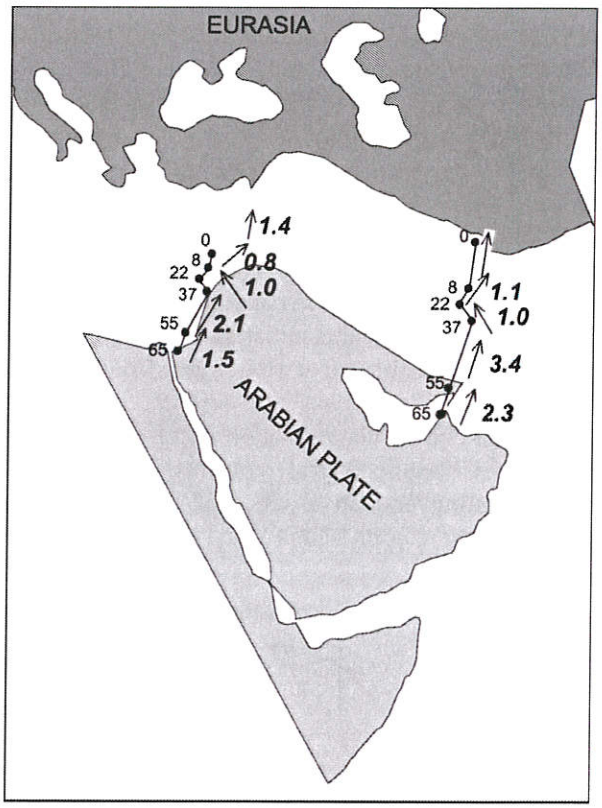

Fig. 3. Cainozoic movements of Arabia relative to Eurasia (after Savostin et al., 1986). Arrows show direction of the movement, small digits show time in Ma, large digits-velocity in cm/year.

Another constraint can be derived from simple area-balancing restoration of the crustal sections (Fig. 2). We used the "equal area" method, i.e. equalise the layer areas of observed crustal section and reconstructed palaeosection. This method is valid in the absence of important lateral displacement between the Scythian and the Transcaucasus plates. Actually, such displacement took place (Philip et al., 1989), but we disregarded it in a first approximation because we are not able to estimate it. A deep water basin similar to the Black Sea and South Caspian basins existed before the collision to the south of the recent GC orogen (Zonenshain and Le Pichon, 1986; Nikishin et al., 1998b). The crustal thickness of this basin is unknown. Crustal thicknesses of the Black Sea and the South Caspian Sea range between 5 and 20 km (Volvovsky et al., 1989) with average values of about 10 km in the Western Black Sea and in the South Caspian Sea, and 15 km in the Eastern Black Sea. The estimated thick-

ness of sediments in the GC trough before the Late Cainozoic collision was about 10 km (e.g. Borsuk and Sholpo, 1983). A simple estimation in the framework of the McKenzie rifting model (by the method of Sclater et al., 1980, for instance), gives a stretching factor $\beta \approx 2.3-2.7$ for 10 km of sediment-filled and 1–2 km of water-filled subsidence in 180 Ma and for 40 km of initial (isostatically and thermally equilibrated) crust which is a typical value for the Scythian Platform. Therefore, the initial thickness of the GC trough crust is estimated at 15–17 km. Consequently, the GC trough crust was not oceanic, but thinned continental crust. This estimation is coherent with the absence of oceanic crustal remnants in the area of underthrusting and an absence of subduction-type volcanism to the north of this area. If we consider these initial crustal thickness values, the Caucasus shortening can be estimated at 200–300 km (Fig. 2), which is in accordance with plate kinematic results and with the opinion of most of the researchers (Khain, 1982; Zonenshain and Le Pichon, 1986; Scherba, 1993; Nikishin et al., 1998b).

Our area-balancing estimations imply also that "full blown" subduction was not manifested during the Late Cainozoic Caucasus collision. Although this collision led to underthrusting and stacking of lithospheric material under the orogen, the slab penetrating into the deep mantle was not developed. As no material escaped into the deep mantle, it is possible to constrain the size of the lithospheric root and, by such a way, to check the capability of the lithospheric root to induce basin subsidence as it was suggested by Ershov et al.

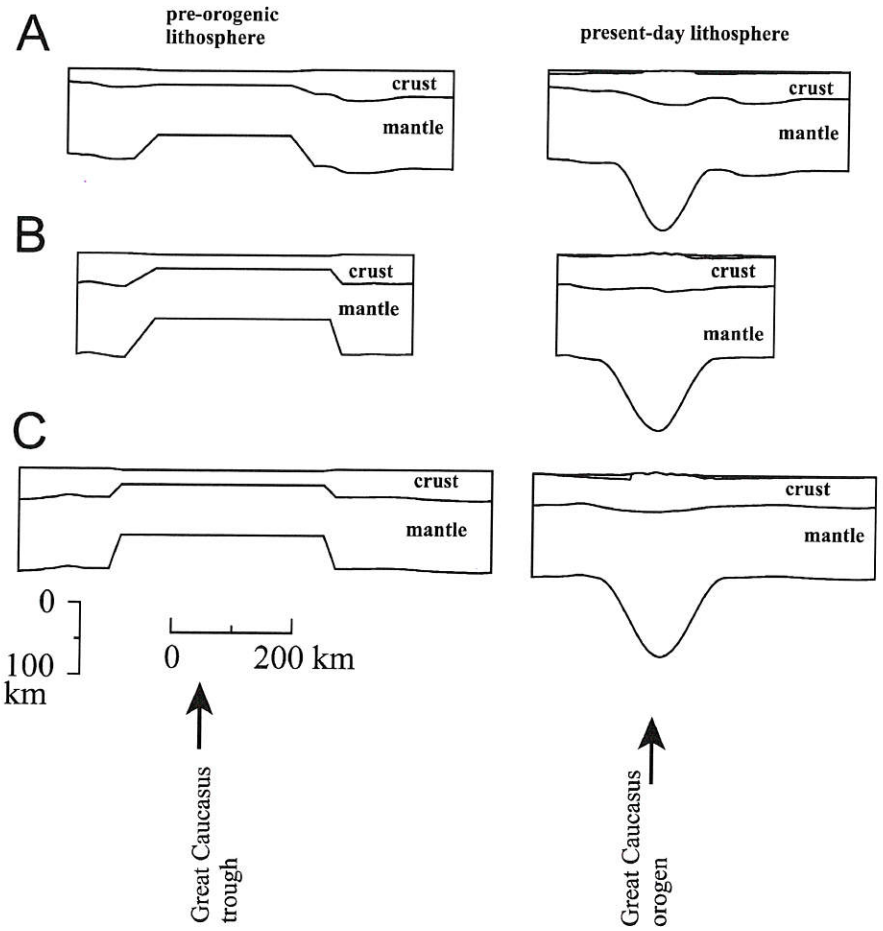

Fig. 4. Sketch showing equal-area estimation of lithospheric thickening and size of lithospheric root. Initial data are results of equal area crustal restorations taking a crustal thickness of 20 km for the basin (Fig. 2). Thickness of lithosphere is estimated on the basis of its thermal age. To be compared with Fig. 9 from Ershov et al. (1999).

(1999) on the basis of gravity and subsidence modelling. The simple estimation is presented in Fig. 4. Comparison with Fig. 9 from Ershov et al. (1999) demonstrates that the size of the lithospheric root is sufficient and, therefore, that the proposed model could "work" indeed in the Caucasus.

3. Burial history of the NCB

3.1. Method

We have used the common backstripping technique (Steckler and Watts, 1978) extended in order to be able to restore 2D seismic sections with compaction correction based on the basin-specific depth-porosity laws (for four basic lithotypes), as well as the eroded parts of the section and to take into account the palaeobathymetry. Details of the method were described elsewhere (Ershov et al., 1998, 1999).

The restoration was made for three 2D geological sections based on the seismic sections and nine wells positioned along the restored sections. The sections and wells were chosen to properly represent the burial history of three major tectonic subdivisions of the NCB: the western, the central and the eastern Fore-Caucasus. The positions of the backstripped wells and seismic sections are shown in Fig. 1a. The chronostratigraphic chart shows the full stratigraphic thickness of the eastern section, and the lithological composition of the sediments is presented by Nikishin et al. (1998a, Fig. 3). The interpretation of the southern lower part of the western section (Fig. 6) is difficult. There are no wells penetrating Jurassic–Cretaceous strata in the area of seismic section. This is the reason why the thickness of Jurassic sediments on the south of the western section was derived from regional-scale interpolation, i.e. interpolating the thickness of the Jurassic layers outcropped in the Caucasus and penetrated by the relatively deep-seated wells (e.g. Borsuk and Sholpo, 1983).

Subsidence curves for the wells are presented in Fig. 5, the western seismic section with elements of interpretation in Fig. 6, and the results of 2D restorations in Fig. 7. These results, together with geological data, are later discussed for each of the principal phases of the basin evolution. The lithological composition and tectonic structure of sediments, as well as subsidence patterns, testify to four major stages: Triassic, Jurassic–Eocene, Oligocene–Early Miocene and Middle Miocene–Quaternary.

3.2. Triassic history

The basement of the NCB is Hercynian in age (Letavin, 1980). It was formed during the Carboniferous–Permian orogeny. An important subsidence event took place in Early–Middle Triassic. This episode is not well known, because most of the Triassic sediments were later removed. Only some folded remnants of Triassic sediments are preserved locally in the former rifts (graben-like structures). The preserved thickness of Early–Middle Triassic sediments is about 3000 m in the western basin and about 1500 m in the central and eastern basins (Letavin, 1988). From the lithological composition of preserved Early–Middle Triassic sediments, it was suggested that the sediments cover the whole territory of the NCB. The in-plane configuration of the Early–Middle Triassic basin is not well established. There exist two points of view (Nazarevich et al., 1983): the first, putting forward that a unique basin covers the whole territory of the Scythian plate, and the second, suggesting two separate basins in the western and the eastern parts subdivided by the central Fore-Caucasus uplift (Stavropol High). The analysis of Early Triassic volcanic rocks shows that the volcanism was related with rifting in back-arc environment (Tikhomirov and Nazarevich, 1999).

Upper Triassic complexes in the eastern basin unconformably overlying older sediments are mainly represented by Late Norian–Rhaetian (Letavin, 1988). The sediments were deposited only in the central part of the eastern basin, whereas the southern and northern parts were folded, uplifted, and eroded. The central and the western basin were also uplifted since about Norian times. It appears that compressional deformation, accompanied by erosion, took place in Late Carnian–Early Norian and in latest Triassic–earliest Jurassic times (Nazarevich et al., 1983). During this time, most of the Triassic sediments were removed in the investigated region. Late Triassic sediments contain a large part of volcanogenic rocks providing evidence that a major volcanic episode took place at this time in the basin. The association of volcanic rocks

is typical for Andean-type continental margins (Tikhomirov and Nazarevich, 1999).

3.3. Jurassic–Eocene history

Two components could be recognised in the Jurassic–Eocene basin subsidence: *regional platform* subsidence and subsidence due to *boundary influence*. The first one extended over large regions and not directly connected with events on the platform boundary. The second was controlled by tectonic events in the surrounding regions, mainly in the southern areas. Geographical sectioning of these two subsidence types determined two major zonations of the basin: longitudinal of *regional* subsidence and latitudinal of *boundary* subsidence.

Three main parts with different *regional* subsidence history could be determined: eastern, central, and western. Regional subsidence began in the eastern area in Late Aalenian, the eastern NCB was covered by sediments first of all—in Bathonian. With time, subsidence and sedimentation gradually extended from east to west and overwhelmed at first the western basin and afterwards; during the Albian, sediments covered the whole territory of the NCB (Fig. 7). The central area was uplifted during whole Jurassic and Early Cretaceous, the sedimentation began only in Late Albian times. During the remaining Cretaceous

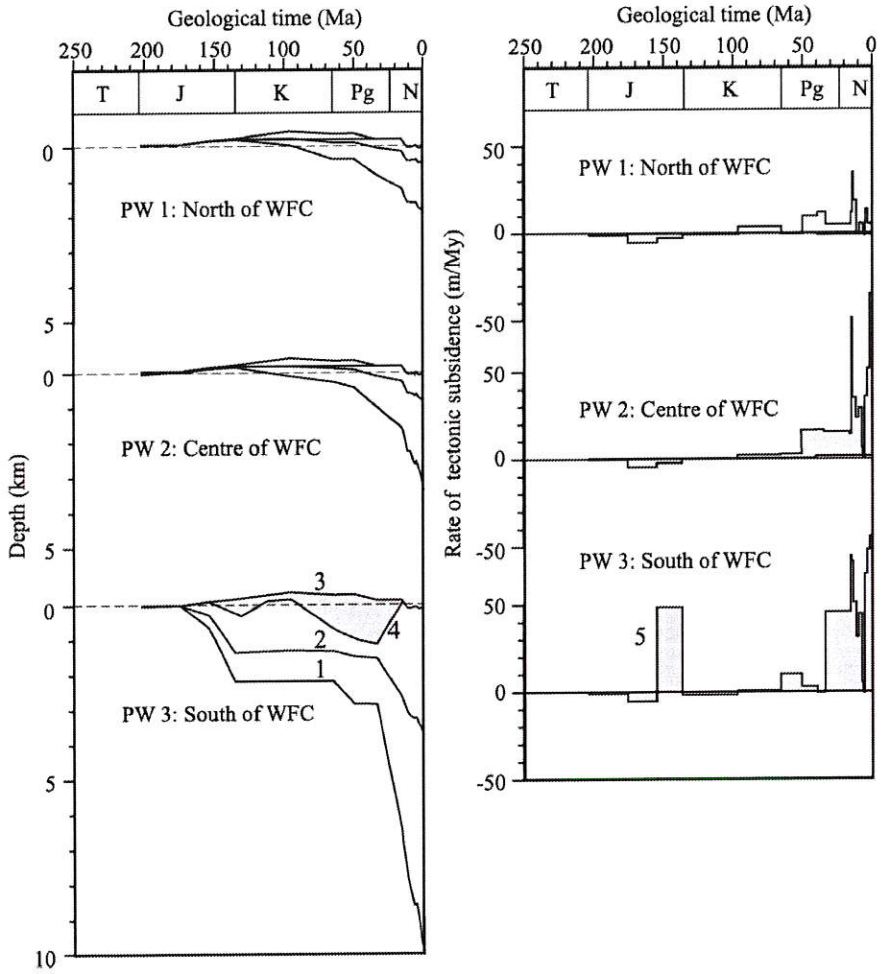

Fig. 5. Late Cainozoic burial histories (1—basement subsidence, 2—air loaded tectonic subsidence, 3—eustatic sea level, 4—palaeobathymetric curve, 5—rate of tectonic subsidence) for nine pseudo-wells (PW) extracted from the modelled seismic sections (Fig. 7) in the Eastern (EFC), Central (CFC) and Western (WFC) Fore-Caucasus. Locations of wells are shown in Fig. 1. Time scale is after Odin (1994).

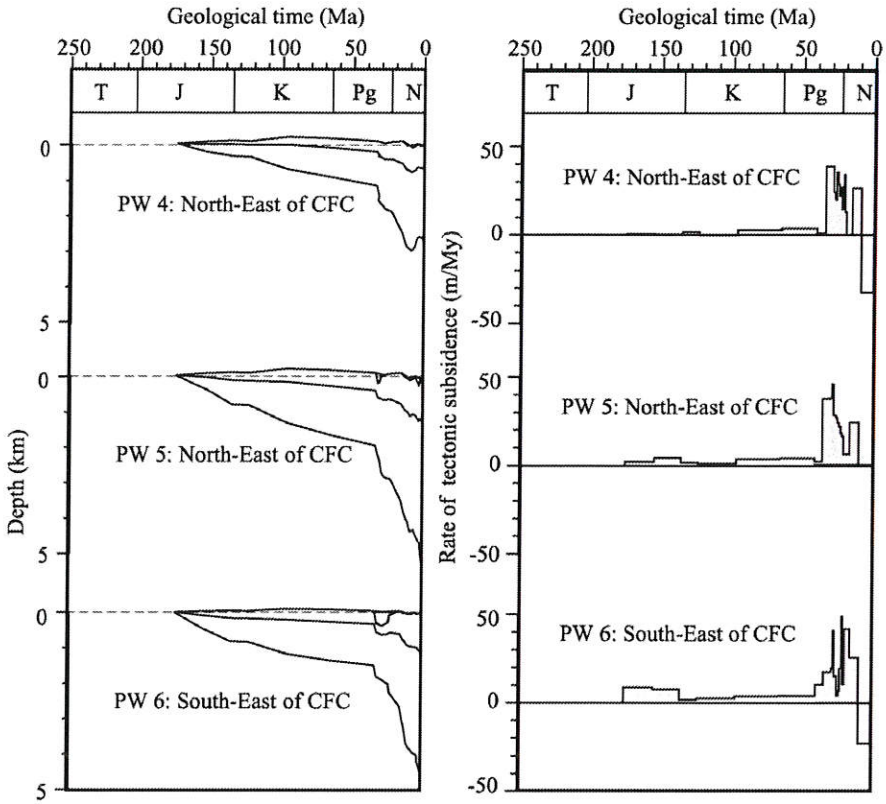

Fig. 5 (*continued*).

until Eocene (135–34 Ma), the subsidence regime in the NCB was quiet and characterised by a decreasing subsidence rate (Fig. 5). The basin was filled by shallow-water carbonates and marls. Subsidence rate was relatively higher in the western and central areas at this time (Fig. 5).

Another subsidence component is associated with the boundary influence of the GC trough. Starting from Early Jurassic (Sinemurian) until Eocene times, the region was a shelf margin of a back-arc basin which was situated on the place of recent GC orogen. The GC basin was formed in the Early Jurassic (Zonenshain et al., 1990; Nikishin et al., 1998a), in a back-arc environment to the north of the Tethyan subduction zone (now situated in the Transcaucasus area). Its northern flank was underthrusted and folded in Middle Jurassic (Bajocian–Bathonian) (Panov and Stafeev, 2000) and in earliest Cretaceous (middle Berriasian) (Mileev et al., 1997, 1998). Each of these minor orogenic events was followed by a renewed stretching. Stress events in the GC influenced the NCB. Proximity to the GC trough determined latitudinal (south–north) sectioning of the basin: proximal areas underwent synrift, postrift and foreland subsidence, whereas distal areas were more or less independent on this influence. The western NCB was also influenced by stress events in the Black Sea area.

Early Jurassic opening of the GC trough was accompanied by a subsidence in the southernmost areas of the NCB (Letavin, 1988). A net of narrow and shallow (several hundred metres) graben-like structures was formed in the eastern NCB during the Sinemurian–Early Aalenian times (Panov and Stafeev, 2000). In the Middle Jurassic (Bajocian–Bathonian), a foreland basin with asymmetrical shape deepening to the GC was formed in the southern areas (Panov and Stafeev, 2000). The thickness of Bajocian–Bathonian sediments in the deepest (southernmost) part is more than 2000 m, whereas in the northern areas of the eastern NCB, which underwent only *regional* subsidence, it is about 500 m. This foreland stage was followed by short uplift and erosion in latest Batho-

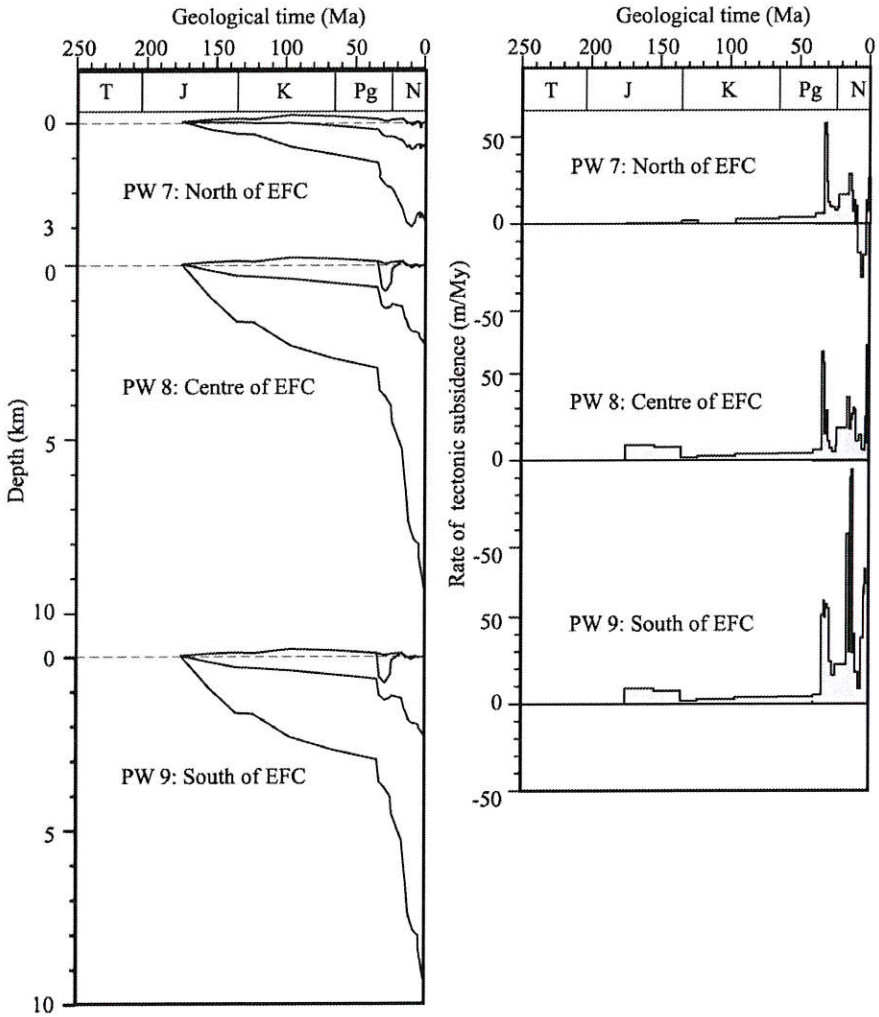

Fig. 5 (*continued*).

nian. The *boundary* subsidence continued in the Callovian following the renewed stretching of the GC trough. The formation of a reef barrier along the southern margin of NCB led to the isolation of the basin and deposition of thick evaporitic sequences in the Late Jurassic.

The next uplift and minor folding event occurred in the earliest Cretaceous (Berriasian), mainly in the western NCB (Figs. 6 and 7). Late Cretaceous and Late Palaeogene episodes of inversion took place also in the western areas (Fig. 6) and were not so pronounced as the Early Cretaceous one.

A rifting episode took place in the central and western areas in Albian times (Fig. 7C). This event is contemporaneous with the opening of the Black Sea, as suggested by Nikishin et al. (2003). Probably at this time, a deep-water non-compensated basin was formed in the southernmost areas (Fig. 7C) of the western NCB as indicated by seismo-stratigraphical analysis of the seismic section (Fig. 6).

3.4. Oligocene–Quaternary history

The Eocene/Oligocene boundary is marked by a rapid broad subsidence of the area and, it also appears, the beginning of a collisional stage continuing until the Present. The lithology of the sediments and the subsidence patterns indicate two main sub-stages: Oligocene–Early Miocene (34–16 Ma) (pre-foreland) and Late Miocene–Quaternary (16–0 Ma) (foreland).

The subsidence history of the NCB during the collisional stage was very complex. It is described in detail by Ershov et al. (1999).

During the first stage a broad deep-water basin was formed in the central-eastern areas. The beginning of the stage is fixed by the change of Upper Eocene shallow water limestones to Oligocene deep water clays. Later, the basin was filled by clinoforms, prograding from the northeast and northwest (Fig. 7A,B). Water palaeodepths, given by our palaeobathymetric estimations and based on the geometrical shape of the clinoforms, are around 500–800 m in the central part and as much as 1200 m in its southern part (Ershov et al., 1998). In general, the subsidence was homogeneous along the basin with a slight tilting to the southeast. Once the basin was filled by the clinoforms, sedimentation continued in shallow-water conditions. The overall thickness of the Maikopian sediments was near 1.7 km in the northern parts, increasing to the southeast (Fig. 7B,C).

The western NCB did not undergo significant tectonic subsidence at the pre-foreland stage. Sediments filled a deep water depression in the southern part of the area (Fig. 7A). Although the subsidence on the shelf was not large, it increased to the south and can be associated with the flexural response of the lithosphere to the loading of sediments, deposited in the deep-water southern part. The overall thickness of the Maikopian sediments in the northern "shelf" part of the section is near 200 m and more than 2000 m in the southern "deep-water" part (Fig. 7A).

The beginning of the next "foreland" stage of the basin evolution is fixed by lithological changes and a subsidence event in the southern areas in the middle Miocene (about 16 Ma). This event marks the beginning of the main collisional phase of the Great Caucasus. This led to the uplift of the western and the eastern segments of the GC orogen (the central segment of the orogen was uplifted already since Late Eocene) above the sea level in the Late Miocene (11 Ma) and also to significant changes of along strike basin configuration at this time. The central area of NCB began to uplift (Fig. 7B) and separated the western and the eastern basins. Subsidence in both basins was asymmetrical with deepening towards the orogen (Fig. 7B,C), typical for foreland basins. The subsidence/sedimentation patterns in the eastern basin were more complex and heterogeneous in comparison with the western one. In particular, amplitude of total uplift of the eastern peripheral bulge was more than 1 km (Fig. 7C), whereas the western bulge was not even elevated above sea level (Fig. 7A) (it occurs only as an area with decreasing thickness of sediments).

4. Thermal evolution of the NCB

Jurassic–Eocene *regional* subsidence of the basin was not large in amplitude, decelerating with time. Subsidence pattern is smooth, subsidence was not fault-controlled. Slow decreasing of subsidence rate with time allows us to suggest a thermal origin of the Jurassic–Eocene *regional* subsidence. To justify this hypothesis, we have carried out thermal modelling of the basin. The basic principles of the adopted thermal model are described in Appendix A.

In general, thermal subsidence results from rock contraction during cooling of the lithosphere after a thermal event. Four basic reasons can induce a thermal event, i.e. heating of the lithosphere: rifting, heating due to increase of mantle or lateral heat flow, intrusive heating and orogeny followed by gravitational spreading of an orogen. The major problems to solve by thermal modelling are: (1) to test the ability of thermal mechanisms to produce observed subsidence pattern, (2) to discriminate between different thermal events and (3) to determine the timing of major thermal events. These problems were examined by comparing theoretically calculated (in the framework of thermal model) tectonic subsidence with backstripped tectonic subsidence.

Tectonic context allows us to put some constraints on the timing of possible thermal events: the major rifting episode in the NCB took place in Early Triassic, the minor rifting—in Early and Late Jurassic (Sinemurian–Aalenian and Callovian) in the eastern area and in Cretaceous (Albian) in the central-western area; a major orogenic event in the NCB took place in Late Triassic; a major magmatic episode also took place in Late Triassic.

Tectonic subsidence derived from a thermal model was compared with averaged tectonic subsidence computed by Bolotov (1996). The results are represented in Fig. 8, parameters of the presented models are displayed in Table 1. Fig. 8a and b demonstrates the net effect of Early Triassic and Early Jurassic

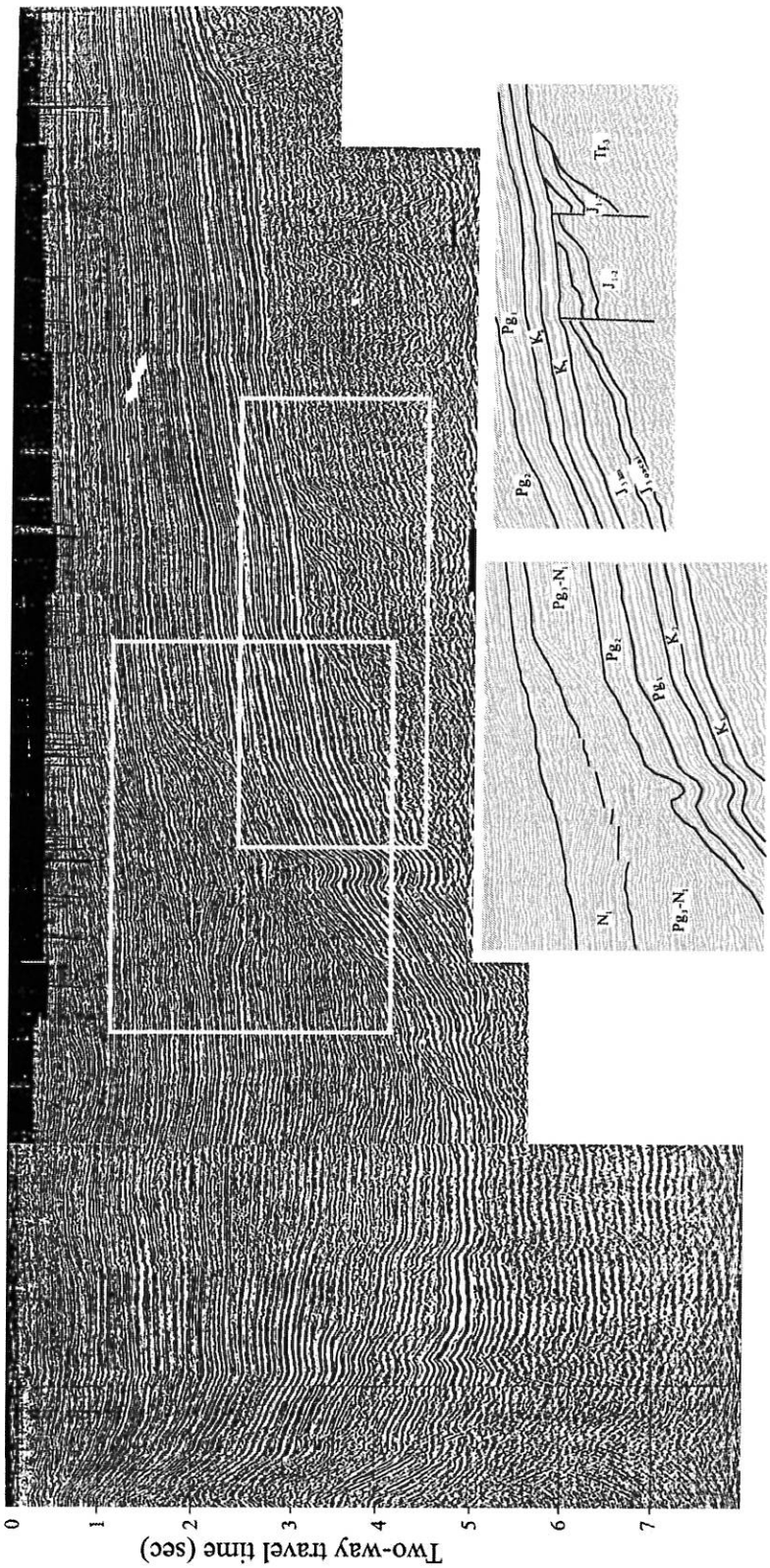

Fig. 6. Seismic section in the Western Caucasus basin. The restoration along the section is presented in Fig. 7. Position of the section is shown in Fig. 1 (section A).

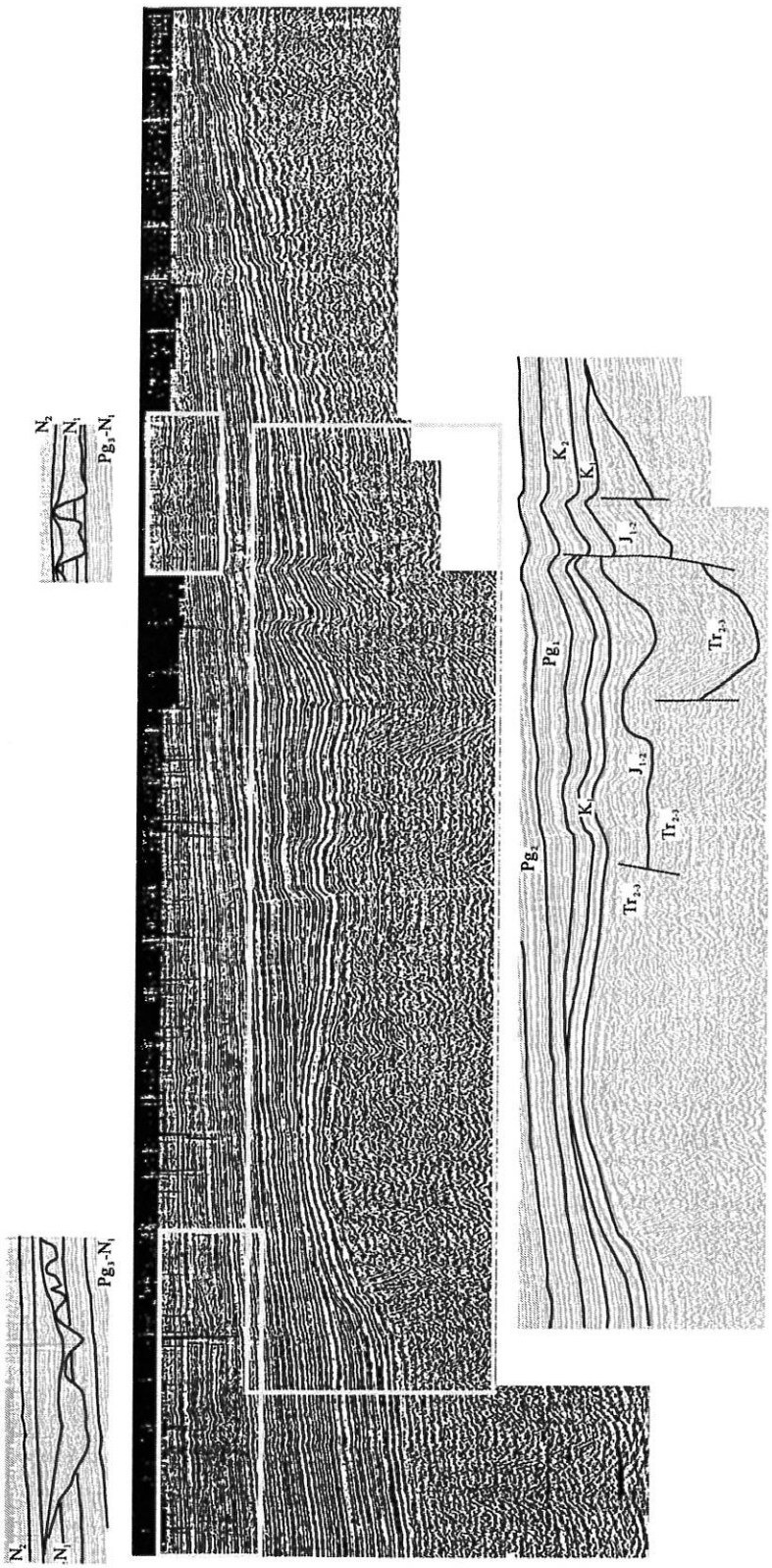

Fig. 6 (*continued*).

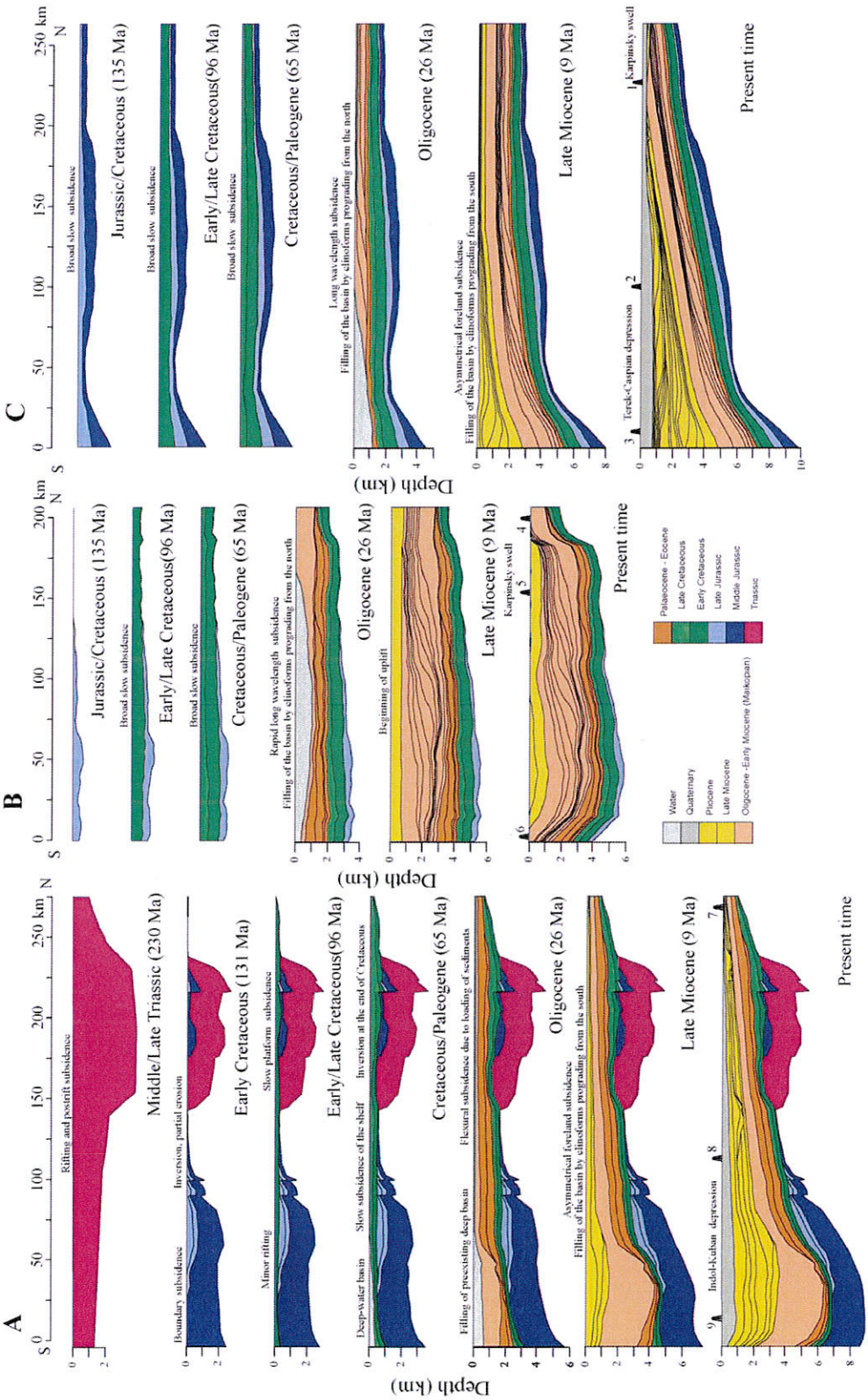

Fig. 7. 2D burial history restoration along the regional seismic sections (black lines on Fig. 1) for some selected time slices. The 1D burial histories for some pseudo-wells are shown in Fig. 5.

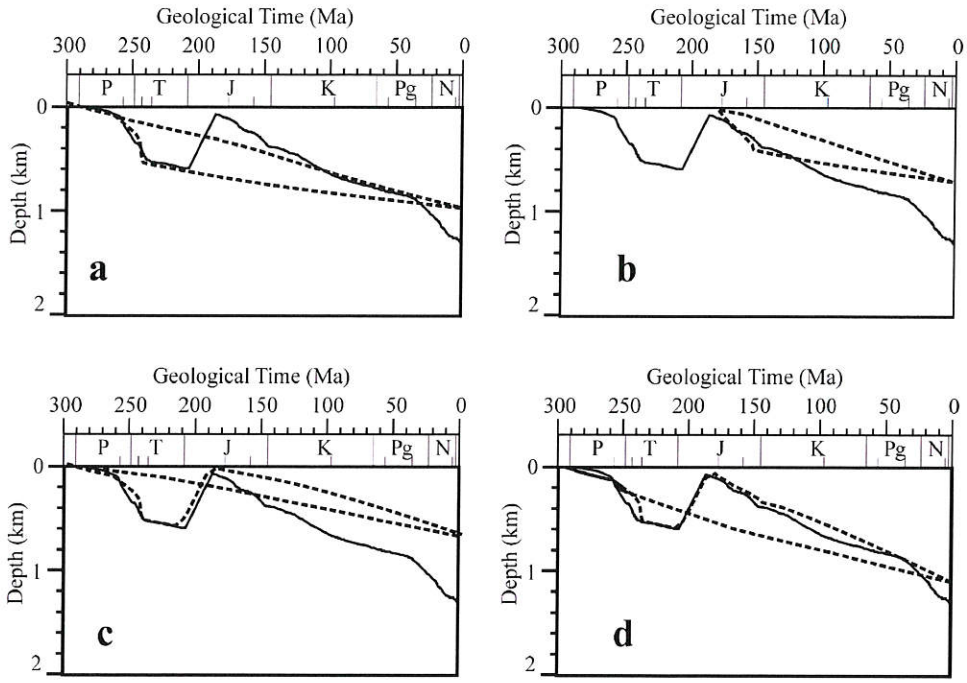

Fig. 8. Results of thermal modelling. Solid line is average tectonic subsidence of the NCB (after Bolotov, 1996), based on 129 backstripped wells. Dashed line is modelled tectonic subsidence. (a) Net effect of Early Triassic rifting. (b) Net effect of Middle–Late Jurassic rifting. (c) Early Triassic rifting and Late Triassic–Early Jurassic heating event. (d) Best-fit model; includes Early Triassic rifting, Late Triassic–Early Jurassic heating event and minor Middle–Late Jurassic rifting.

rifting. Apparently rifting cannot explain Late Triassic–Early Jurassic regional uplift. This uplift can be explained by Late Triassic volcanic episode, which induces heating of the lithosphere and thermal doming. The effect of Early Triassic rifting followed by Late Triassic–Early Jurassic heating event is shown in Fig. 8c. However, cooling rate in this case is not sufficient to produce observed subsidence rate in Late Jurassic–Eocene. Fig. 8d demonstrates the best-fit model. It includes Early Triassic rifting, Late Triassic–Early Jurassic magmatic heating and Middle–Late Jurassic rifting. The thinning factor of the Jurassic rifting in the best-fit model is only 1.05.

We conclude that a thermal mechanism is capable of explaining the general trend of the Triassic–Eocene basin subsidence and that the two most probable subsidence-controlling thermal events are an Early Triassic rifting followed by a Late Triassic magmatic heating of the lithosphere. This induced Late Triassic–Early Jurassic thermal uplift and erosion and subsequently long wavelength thermal subsidence of the whole basin. Minor Mid–Late Jurassic rifting is also necessary to explain observed subsidence rate.

Table 1
Parameters of the thermal models presented

Figure	Rifting events		Magmatic events		
	Time of rifting (Ma)	Thinning factor (β)	Time of intrusions (Ma)	Melt amount (%)	Bottom heat flux increase (mW/m^2)
8a	253–244	1.5	–	–	–
8b	194–187	1.1	–	–	–
8c	253–244	1.5	210–190	19	50
8d	253–244	1.5	210–190	19	50
	194–187	1.1			

5. Conclusion: synthesis of basin subsidence models

Subsidence of the Northern Caucasus basin cannot be explained by a single model but was controlled by

different mechanisms replacing each other during the basin evolution. Here we present a synthesis of the basin subsidence models in a regional tectonic context (Fig. 9), which was mainly determined by the Tethyan subduction and induced opening and closure of back-arc basins. The correlation of events in the Northern Caucasus basin, in the Great Caucasus and in the area of Tethyan subduction is displayed in Table 2.

Subsidence of the basin started in Early Triassic times due to gravitational spreading of the Late Palaeozoic Scythian orogen. Sediments were deposited, at the beginning in grabens, and later, covered the whole territory of the former orogen. Thickness of sedimentary cover was about 2–3 km. In the Late Triassic, due to collision of the Transcaucasus terrane with the Scythian Platform, the sedimentary cover was folded and mostly eroded. It was the time of the Eocimmerian collision, when Gondwana terranes collided with Eurasian plate. The lithosphere of the basin was heated by numerous intrusions. This heating led to thermal uplift of the whole area and erosion of Triassic sediments. Later on, the lithosphere began to cool and subside and this thermal contraction of the lithosphere controlled the basin subsidence (during Jurassic to Eocene times), according to the thermal modelling presented in this paper.

In Early Jurassic times (in Sinemurian), the Great Caucasus back-arc basin opened further to the south. This led to subsidence in the southernmost areas of the Northern Caucasus basin adjacent to the Great Caucasus trough and induced minor rifting in the northern areas, superimposed on regional uplift background. In Middle Jurassic (Bajocian–Bathonian), the northern slope of the Great Caucasus trough was underthrusted and this minor "orogeny" induced foreland subsidence on the south of the NCB during Bajocian–Bathonian times. At the end of this "orogenic" stage, the basin was unflexed and partly eroded. The Great Caucasus basin continued to spread during Callovian times. Starting from this time until the Miocene, the Northern Caucasus basin was geographically a shelf part of the Great Caucasus deep-water trough. The major subsidence-driving mechanism was thermal cooling of the lithosphere. Second-order stress events in the Great Caucasus trough determined the second-order subsidence rate variations in the NCB. Minor orogeny in the Western Caucasus at Jurassic/Cretaceous boundary induced thrusting, differential uplift and partial erosion in the Western Caucasus basin at this time. A consequent Aptian–Albian extensional event in the west, followed by the opening of the Black Sea, induced minor rifting in the central and western NCB and deepening of the southernmost parts of the western NCB. This area remained underfilled by sediment until the end of Palaeogene.

The next stage began in latest Eocene when Arabia collided with Eurasia. The GC trough began to close, at the same time that the eastern and central areas of the NCB (as well as Central Caspian and Turkmenian basins, which we did not considered here) underwent an episode of rapid long wavelength subsidence. The mechanism of this subsidence is unclear. However, the characteristic wavelength of the subsidence points out that its cause should lie amongst large-scale processes, such as mantle convection. The analysis of Late Eocene–Early Oligocene collisional settings allows this subsidence to be associated with the termination of subduction in the southern areas. If so, its cause may be the mantle flow induced by reequilibration of the subducted slab after cessation of subduction. This subsidence is, therefore, "dynamically supported" and it should lead to uplift upon its cessation. However, in the eastern area, the implied uplift stage appears to have been masked by the foreland subsidence of the next stage of basin development.

The Caucasus orogeny came to its major phase in middle Miocene (this is the time of final closure of the Great Caucasus trough). Since this time the Northern Caucasus basin has undergone asymmetrical foreland-type subsidence. According to flexural modelling (Ershov et al., 1999), the major subsidence-controlling factors were crustal and lithospheric thickening and removal of lithospheric root (Fig. 10). Observed 3D-subsidence pattern results from superposition of these factors. Loading due to the presence of lithospheric root has induced subsidence of the basin and, in particular, deep subsidence at the tips of the orogen. The estimation of the lithospheric root size presented in Fig. 4 being compared with the flexural modelling results (Ershov et al., 1999, Fig. 9) demonstrates that the amount of this loading is sufficient. Removal of the lithospheric root, in combination with crustal thickening, explains the uplift of the central Northern Caucasus area. This point is supported by seismotomographic data (Brunet et al., 2000). Highly elevated topography appears in the Central Caucasus orogen only at the

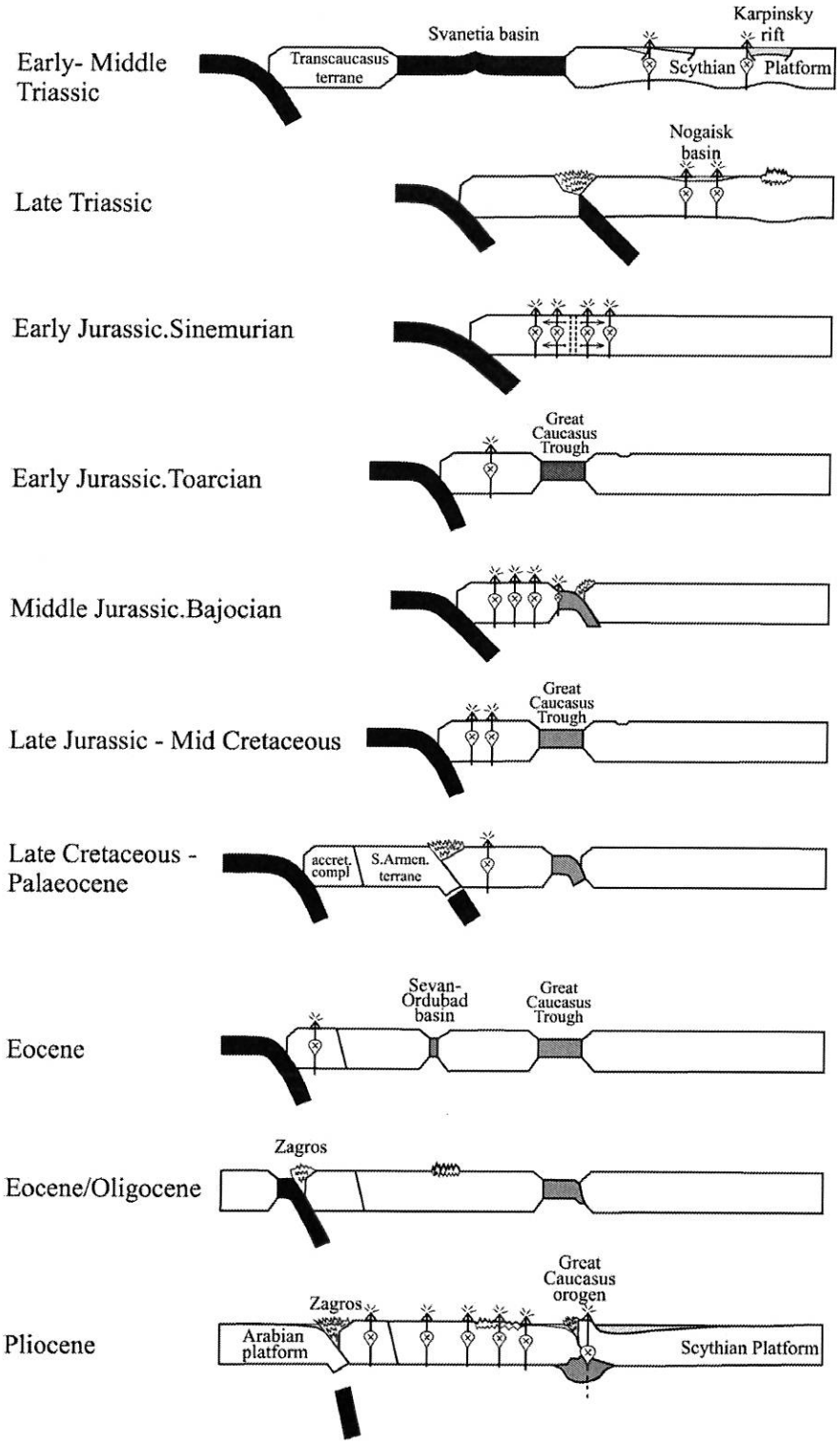

Fig. 9. Schematic tectonic reconstruction, showing tectonic environments of the area since the Triassic time.

Table 2
Correlation of the events in the region. Absolute age after Harland et al. (1989) and Odin (1994)

Geological Age							Tethyan subduction zone	Great Caucasus (GC)	Northern Caucasus Basin (NCB)		
Relative					Absolute (Ma) Harland, 1989	Absolute (Ma) Odin, 1994			Western	Central	Eastern
Quaternary					1.64	1.75	Collisional climax	Rapid uplift	Foreland-type subsidence	Uplift and erosion	Beginning of unflexing
Cenozoic	Neogene	Pliocene	Piacenzian	Akchagylian	3.4	3.4		Major orogenic phase, propagation of orogeny from the center to the east and to the west			Foreland-type subsidence, large erosion of peripheral bulge
			Zancleian	Kimmerian	5.2	5.3					
		Miocene	Messinian	Pontian	6.7	7.1					
			Tortonian	Meotian 9.3					Foreland-type subsidence		
				Sarmatian 13.7	10.4	11					
			Serravalian	Konkian	14.2	14.7	Collision of Arabia with Eurasia	Beginning of orogeny in the central area			
			Langhian	Karaganian Chokrakian	16.3	15.8					
			Burdigalian	Tarkhanian 17	21.5	20.3			Filling of pre-existing basins by sediments	Rapid long wavelength subsidence	
			Aquitanian	Maikopian	23.3	23					
	Palaeogene	Oligocene	Chattian		29.3	28					
			Rupelian		35.4	33.7					
		Eocene	Priabonian		38.6	37	Tethyan subduction	Stretching in the Eastern Black Sea	Post-rift subsidence, formation of deep-water non-compensated basin in the south, slow platform subsidence in the north	Post-rift subsidence	Slow regional thermally-driven subsidence
			Bartonian		42.1	40					
			Lutetian		50	46					
			Ypresian		56.5	53					
		Paleocene	Thanetian		60.5	59	Terranes accretion and orogeny in Turkey. Initiation of new subduction in Zagros	Compressive phase (?) in the west			
			Danian		65	65					
Mesozoic	Cretaceous	Late	Maastrichtian		74	72					
			Campanian		83	83					
			Santonian		86.6	87	Tethyan subduction	Opening of the Black Sea			
			Coniacian		88.5	88					
			Turonian		90.4	92					
			Cenomanian		97	96			rifting, volcanism		
		Early	Albian		112	108					
			Aptian		124.5	113			Slow regional subsidence	Regional uplift	
			Barremian		131.8	117					
			Hauterivian		135	123					
			Valanginian		140.7	131					
			Berriasian			135		Compressional event	Folding, uplift, erosion		
	Jurassic	Malm	Tithonian		152.1	141		Renewed stretching of the GC trough	Slow regional subsidence		
			Kimmeridgian		154.7	146					
			Oxfordian		157.1	154					
		Dogger	Callovian		161.3	160			short uplift		short uplift
			Bathonian		166.1	164		"Orogeny", partial closure of the GC trough	Foreland subsidence in the south		Foreland subsidence in the south
			Bajocian		173.5	170					
		Lias	Aalenian		178	175	Initiation of new subduction	Opening of the GC trough along volcanic arc	Regional thermal uplift, subsidence in the southernmost areas, minor rifting		
			Toarcian		187	184					
			Pliensbachian		194.5	191		Volcanic arc			
			Sinemurian		203.5	200					
			Hettangian		208	203	Collision of Gondwanian terranes with Eurasia	Orogeny	Uplift, volcanism		Orogeny to the north and to the south, subsidence in the center
	Triassic	Late	Rhaetian		209.5	--					
			Norian		223.4	220					
			Carnian		235	230					
		Mid	Ladinian		239.5	233	Palaeo-Tethyan subduction	Opening of the Svanetia trough in back-arc environment	post-rift subsidence		
			Anisian		241.1	240					
		Early	Olenekian			--			Gravitational collapse of the orogen, back-arc rifting, rift-related volcanism		
			Indusian		245	250					
	Permian							Andean-type orogeny	Orogeny, denudation, narrow basins filled by molasse		

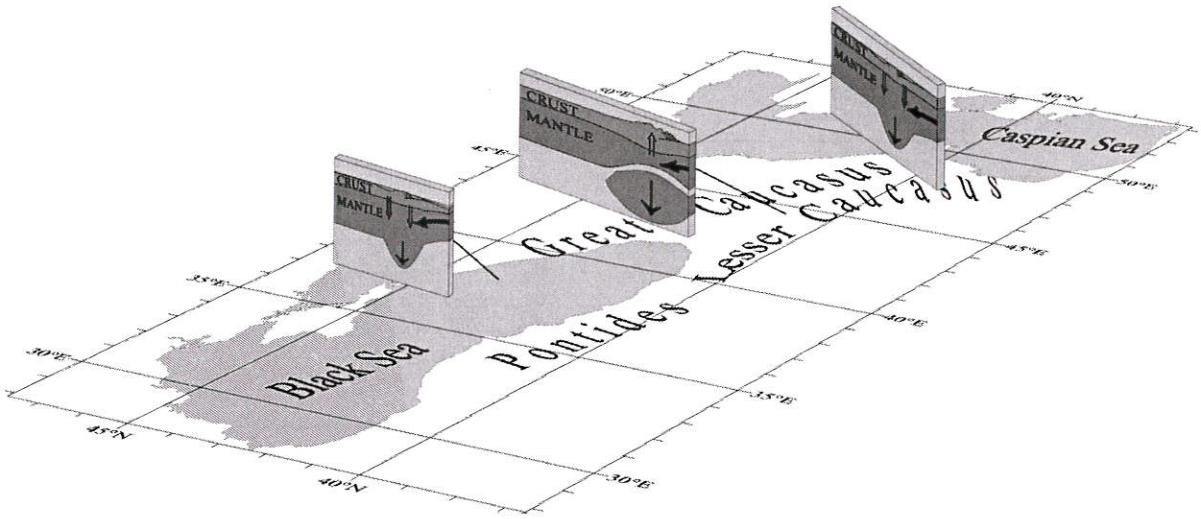

Fig. 10. Sketch showing the main subsidence-driving mechanisms for the foreland stage of basin evolution in different areas of the Caucasus.

final stages of evolution, following removal of lithospheric root.

Acknowledgements

This work was funded by the Peri-Tethys Programme and INTAS. The international programmes Europrobe and Lithosphere supported our communications and discussions. We are grateful to A.F. Morozov and the Russian Geological Survey for supporting our work. Thanks are also due to V.E. Khain, H. Philip and E.B. Burov for their constructive reviews, and to E.Yu. Baraboshkin, J. Dercourt, S.S. Kosova, E.E. Milanovsky, D.I. Panov, R. Stephenson, P.L. Tikhomirov and P. Ziegler for their fruitful discussions.

Appendix A. Thermal model

We solved the inverse thermal problem by the "trial-and-error" method, i.e. repeatedly solving the forward problem with changing inputs until reaching the best-fit with observations (until the best-fit between calculated subsidence in the framework of the thermal model and backstripped subsidence).

As a general rule, the basic principles of the used thermal model are similar to those of the model presented by Monzer et al. (1998). The model is based on the implicit finite-difference solution of 1D heat transfer equation

$$\frac{\partial(\rho C_p T)}{\partial t} = \frac{\partial}{\partial z}\left(k\frac{\partial T}{\partial z}\right) + A$$

with adaptive mesh size and time step. Designations and values of material parameters are displayed in Table 3. The numerical scheme was tested on known analytical solutions.

The calculation area extends up to 200 km downward. Initial thickness of the crustal layers was derived from the observed one multiplying by the total thinning factor.

A constant surface temperature of 20 °C was used as an upper boundary condition. The second boundary condition was heat flow on the lower boundary of calculation area. Time-dependent value of heat flow was varied in the ranges constrained by the tectonic context to obtain the best-fit. Steady-state temperature distribution was used as an initial boundary condition.

Rifting was simulated by means of McKenzie-type algorithm: at each time step during the rifting period, the size of each cell was decreased by the value derived from the thinning factor. The thinning factor of each rifting period was varied to obtain the best-fit. Timing and duration of rifting stages were determined from geological data. Isostatic reequilibration after decreasing of cell sizes leads to isostatic subsidence,

Table 3
Parameters used in the thermal modelling

Parameter	Designation	Upper crust	Lower crust	Mantle	Measurement unit
Depth	z	0–20	20–40	40–200	km
Density	ρ	2.8	2.9	3.3	$g\ m^{-3}$
Thermal conductivity	k	2.7	3.0	3.5	$W\ m^{-1}\ K^{-1}$
Specific heat capacity	ρC_p	2.8	3.0	3.5	$10^6\ J\ m^{-3}\ K$
Heat production	A_0	2.0	2.0	0	$10^{-6}\ W\ m^{-3}$
$A=A_0 \exp(-z/h_r)$	h_r	10	10	–	km
Thermal expansion coefficient	α	2	2	2	$10^{-5}\ K^{-1}$

which was calculated supposing equality of weights of lithospheric columns before and after stretching. Thermal expansion and contraction were computed at each time step for each cell as

$$\delta(\Delta z) = \alpha \Delta T$$

where ΔT is the temperature change and $\delta(\Delta z)$ is the change of cell size. Total thermal subsidence is equal to the sum of cell sizes changes. Basin subsidence was taken as a sum of subsidence due to stretching and due to thermal contraction. To simplify calculations, we did not take into account sedimentation and, by such a way, air-loaded tectonic subsidence was calculated. The composition and structure of the sedimentary cover influence temperatures mainly in sediments. Thermal subsidence depends mainly on crustal and mantle temperatures and, therefore, the thermal influence of the sedimentary cover is not significant for our purposes and can be neglected.

Intrusive heating of the lithosphere was modelled by uniform adding of certain amount of the melt at 1300 °C to the lithospheric column. This increases temperature and size of each cell. The amount of the intruded melt determined the amount of added heat through melt heat capacity whose value was taken as $3.10^6\ J\ m^{-3}\ K$. The amount of intruded melt was varied to reach the best fit with observation.

The adopted model is one-dimensional and possesses some limitations. In particular, the temperature changes due to lateral heat flux were not taken into account. This factor is important for the subsidence of the boundary areas of the NCB adjacent to GC trough. However, for *regional* subsidence (i.e. subsidence of large area), which we model, this influence is negligible.

References

Adamia, S., Akhvlediani, K.T., Kilasonia, V.M., Nairn, E.M., Papava, D., Patton, D., 1992. Geology of the republic of Georgia: a review. International Geology Review 34, 447–476.

Artyushkov, E.V., 1993. Physical Tectonics. Nauka, Moscow, 456 pp. In Russian.

Bazhenov, M.L., Burtman, V.S., 1990. Structural Arcs of the Alpine Belt: Carpathians, Caucasus, Pamir. Nauka, Moscow, 165 pp. In Russian.

Bolotov, S.N., 1996. Mesozoic–Cenozoic history of Scythian Platform and numerical characteristics of basic stages of evolution on the base of computer modelling. Ph.D. Thesis, Lomonosov Moscow State University, Geological Faculty, Moscow, 195 pp. In Russian.

Borsuk, A.M., Sholpo, V.N., 1983. Correlation of endogenic processes in the Alpine cycle of the Caucasus. In: Rast, N., Delany, F.M. (Eds.), Profile of Orogenic Belts. American Geophysical Union, Geodynamic Series, Washington D.C., vol. 10, pp. 97–143.

Brunet, M.-F., Spakman, W., Ershov, A.V., Nikishin, A.M., 2000. Information given by the tomography on the geodynamics of the Caucasus–Caspian area. European Geophysical Society Meeting, Nice, France, 25–29 April.

Brunet, M.-F., Korotaev, M., Ershov, A.V., Nikishin, A.M., 2003. The South Caspian basin: a review of its evolution from subsidence modelling. In: Brunet, M.-F., Cloetingh, S. (Eds.), Integrated Peri-Tethyan Basin Studies (Peri-Tethys Programme). Sedimentary Geology, this issue.

De Mets, C., Gordon, R.G., Argus, D.F., Stein, S., 1990. Current plate motions. Geophysical Journal International 101, 425–478.

Ershov, A.V., Brunet, M.-F., Nikishin, A.M., Bolotov, S.N., Korotaev, M.V., Kosova, S.S., 1998. Evolution of the eastern Fore-Caucasus basin during the Cenozoic collision: burial history and dynamic modelling. In: Crasquin-Soleau, S., Barrier, E. (Eds.),

Peri-Tethys Memoir 4: Epicratonic Basins of Peri-Tethyan Platforms. Mémoires du Muséum National d'Histoire Naturelle, Paris, vol. 179, pp. 111–130.

Ershov, A.V., Brunet, M.-F., Korotaev, M.V., Nikishin, A.M., Bolotov, S.N., 1999. Late Cenozoic burial history and dynamics of the Northern Caucasus molasse basin: implications for foreland basin modelling. In: Stephenson, R.A., Wilson, M., Starostenko, V.I. (Eds.), EUROPROBE Georift. Vol. 2: Intraplate Tectonics and Basin Dynamics of the Eastern European Craton and its Margins. Tectonophysics, vol. 313, pp. 219–241.

Gamkrelidze, I.P., 1986. Geodynamic evolution of the Caucasus and adjacent areas in Alpine time. Tectonophysics 127, 261–267.

Harland, W.B., Armstrong, R.L., Cox, A.V., Craig, L.E., Smith, A.G., Smith, D.G., 1989. A Geologic Time Scale. Cambridge Univ. press, Cambridge, 263 pp.

Khain, V.E., 1982. Comparison of fixist and mobilist models of the tectonic evolution of the Greater Caucasus. Geotectonics 16, 249–257.

Kopp, M.L., Scherba, I.G., 1998. Caucasian basin in the paleogene. Geotectonics 32, 93–113.

Krasnopevtseva, G.V., 1984. Deep Structure of the Caucasus Seismoactive Region. Nauka, Moscow, 107 pp. In Russian.

Letavin, A.I., 1980. Basement of the Young Platform of the Southern Part of USSR. Nauka, Moscow, 153 pp. In Russian.

Letavin, A.I. (Ed.), 1988. Mesozoic and Cenozoic Complexes of the Fore-Caucasus (Structure and Correlation). Nauka, Moscow, 92 pp. In Russian.

McClusky, S., Balassanian, S., Barka, A., Demir, C., Ergintav, S., Georgiev, I., Gurkan, O., Hamburger, M., Hurst, K., Kahle, H., Kastens, K., Kekelidze, G., King, R., Kotzev, V., Lenk, O., Mahmoud, S., Mishin, A., Nadariya, M., Ouzounis, A., Paradissis, D., Peter, Y., Prilepin, M., Reilinger, R., Sanli, I., Seeger, H., Tealeb, A., Toksoz, M.N., Veis, G., 2000. Global positioning system constraints on plate kinematic and dynamics in the eastern Mediterranean and Caucasus. Journal of Geophysical Research 105, 5695–5719.

Mikhailov, V.O., 1993. Crustal control on the Terek-Caspian trough evolution: constraints based on a new paleotectonic analysis method. Tectonophysics 238, 21–32.

Mikhailov, V.O., Panina, L.V., Polino, R., Koronovsky, N.V., Kiseleva, E.A., Klavdieva, N.V., Smolyaninova, E.I., 1999a. Evolution of the North Caucasus foredeep: constraints based on the analysis of subsidence curves. Tectonophysics 307, 361–379.

Mikhailov, V.O., Timoshkina, E.P., Polino, R., 1999b. Foredeep basins: the main features and model of formation. Tectonophysics 307, 345–359.

Mileev, V.S., Rozanov, S.B., Baraboshkin, E.Yu., Shalimov, I.V., 1997. Geological structure and evolution of Mountain Crimea. Vestnik MGU, Ser. Geologicheskaya 3, 17–21 (in Russian).

Mileev, V.S., Rozanov, S.B., Baraboshkin, E.Yu., Shalimov, I.V., 1998. Peculiarities of internal deformation of Mountain Crimea allochtones. Doklady Rossiiskoi Academii Nauk 358, 233–235 (in Russian).

Monzer, M., Galushkin, Yu.I., Lopatin, N.V., 1998. Burial history and kinetic modelling for hydrocarbon generation: Part I. The GALO model. American Association of Petroleum Geologists Bulletin 81, 1660–1678.

Nazarevich, B.P., Nazarevich, I.A., Shvydko, N.I., 1983. Lower Triassic sediments of the Scythian Platform—formations and oil potential. In: Vassoevich, B.P., Timofeev, P.P. (Eds.), Sedimentary Basins and their Hydrocarbon Potential. Nauka, Moscow, pp. 123–151. In Russian.

Nikishin, A.M., Ziegler, P.A., Stephenson, R.A., Cloetingh, S.A.P.L., Furne, A.V., Fokin, P.A., Ershov, A.V., Bolotov, S.N., Korotaev, M.V., Alekseev, A.S., Gorbachev, V.I., Shipilov, E.V., Lankreijer, A., Bembinova, E.Yu., Shalimov, I.V., 1996. Late Precambrian to Triassic history of the East-European Craton: dynamics of sedimentary basin evolution. Tectonophysics 268, 23–63.

Nikishin, A.M., Cloetingh, S., Bolotov, S.N., Baraboshkin, E.Y., Kopaevich, L.F., Nazarevich, B.P., Panov, D.I., Brunet, M.-F., Ershov, A.V., Il'ina, V.V., Kosova, S.S., Stephenson, R.A., 1998a. Scythian platform: chronostratigraphy and polyphase stages of tectonic history. In: Crasquin-Soleau, S., Barrier, E. (Eds.), Peri-Tethys Memoir 3: Stratigraphy and Evolution of Peri-Tethyan Platforms. Mémoires du Muséum National d'Histoire Naturelle, Paris, vol. 177, pp. 151–162.

Nikishin, A.M., Cloetingh, S., Brunet, M.-F., Stephenson, R., Bolotov, S.N., Ershov, A.V., 1998b. Scythian Platform and Black Sea region: Mesozoic–Cenozoic tectonic and dynamics. In: Crasquin-Soleau, S., Barrier, E. (Eds.), Peri-Tethys Memoir 3: Stratigraphy and Evolution of Peri-Tethyan Platforms. Mémoires du Muséum National d'Histoire Naturelle, Paris, vol. 177, pp. 163–176.

Nikishin, A.M., Korotaev, M.V., Ershov, A.V., Brunet, M.-F., 2003. The Black Sea Basin: tectonic history and Neogene–Quaternary rapid subsidence modelling. In: Brunet, M.-F., Cloetingh, S. (Eds.), Integrated Peri-Tethyan basin studies (Peri-Tethys Programme). Sedimentary Geology, this issue.

Odin, G.S., 1994. Geological time scale. Comptes Rendus de l'Académie des Sciences. Série II 318, 59–71.

Panov, D.I., Stafeev, A.N., 2000. Early and Middle Jurassic of the Scythian and Turanian plates. Vestnik MGU Ser. 4 Geologia 2, 1–20 (in Russian).

Philip, H., Cisternas, A., Gvishiani, A., Gorshkov, A., 1989. The Caucasus: an actual example of the initial stages of continental collision. Tectonophysics 161, 1–21.

Reilinger, R.E., McClusky, S.C., Oral, M.B., King, R.W., Toksoz, M.N., Barka, A.A., Kinik, I., Lenk, O., Sanli, I., 1997a. Global positioning system measurements of present-day crustal movements in the Arabia–Africa–Eurasia plate collision zone. Journal of Geophysical Research 102, 9983–9999.

Reilinger, R.E., McClusky, S.C., Souter, B.J., Hamburger, M.W., Prilepin, M.T., Mishin, A., Guseva, T., Balassanian, S., 1997b. Preliminary estimates of plate convergence in the Caucasus collision zone from global positioning system measurements. Geophysical Research Letters 24, 1815–1818.

Robinson, A.G., Rudat, J.H., Banks, C.J., Wiles, R.L.F., 1996. Petroleum geology of the Black Sea. Marine and Petroleum Geology 13, 195–223.

Ruppel, C., McNutt, M., 1990. Regional compensation of the Great Caucasus mountains based on an analysis of Bouguer gravity data. Earth and Planetary Science Letters 98, 360–378.

Savostin, L.A., Sibuet, J.-C., Zonenshain, L.P., Le Pichon, X., Roulet, M.-R., 1986. Kinematic evolution of the Tethys belt

from the Atlantic ocean to the Pamir since the Triassic. Tectonophysics 123, 1–35.

Scherba, L.G., 1993. Stages and Phases of Cenozoic Development of Alpine Fold Belt. Nauka, Moscow, 231 pp. In Russian.

Sclater, J.G., Jaupart, C., Galson, D., 1980. The heat flow through oceanic and continental crust and the heat loss of the Earth. Reviews of Geophysics and Space Physics 18, 269–311.

Smith, D.E., Kolenkiewics, R., Robbins, J.W., Dunn, P.J., Torrence, M.H., 1994. Horizontal crustal motion in the central and eastern Mediterranean inferred from satellite laser ranging measurements. Geophysical Research Letters 21, 1979–1982.

Steckler, M.S., Watts, A.B., 1978. Subsidence of the atlantic-type continental margin off New York. Earth and Planetary Science Letters 41, 1–13.

Tikhomirov, P.L., Nazarevich, B.P., 1999. Triassic volcanic activity in the Eastern Fore-Caucasus (Scythian platform): new data on the problem of North-Tethys volcanic belt. Europrobe meeting, Tulcea, Romania, September 25–October 6, Abstracts. Romanian Journal of Tectonics and Regional Geology 77/1, 84.

Volvovsky, I.S., Moskalenko, V.N., Neprochnov, Yu.P., Shlezinger, A.E., 1989. Thickness and structure of the consolidated crust. In: Belousov, V.V., Volvovsky, B.S. (Eds.), Structure and Evolution of the Earth's Crust and Upper Mantle of the Black Sea. Nauka, Moscow, pp. 136–138. In Russian.

Westphal, M., Bazhenov, M.L., Lauer, J.P., Pechersky, D.M., Sibuet, J.-C., 1986. Paleomagnetic implications on the evolution of the Tethys belt from the Atlantic ocean to the Pamirs since the Triassic. Tectonophysics 123, 37–82.

Zonenshain, L.P., Le Pichon, X., 1986. Deep basins of the Black Sea and Caspian Sea as remnants of Mesozoic back-arc basins. Tectonophysics 123, 181–211.

Zonenshain, L.P., Kuzmin, M.I., Natapov, L.M., 1990. Geology of the USSR: a plate tectonic synthesis. American Geophysical Union, Geodynamic Series, Washington D.C., vol. 21. 242 pp.